

2016

The C-terminal motif of SiAGO1b is required for the regulation of growth, development and stress responses in foxtail millet (*Setaria italica* (L.) P. Beauv)

Xiaotong Liu
Chinese Academy of Agricultural Sciences


Sha Tang
Chinese Academy of Agricultural Sciences

Guanqing Jia
Chinese Academy of Agricultural Sciences

James C. Schnable
University of Nebraska-Lincoln, schnable@unl.edu

Haixia Su
Chinese Academy of Agricultural Sciences

Follow this and additional works at: <https://digitalcommons.unl.edu/agronomyfacpub>

 [next page for additional authors](#)
Part of the [Agricultural Science Commons](#), [Agriculture Commons](#), [Agronomy and Crop Sciences Commons](#), [Botany Commons](#), [Horticulture Commons](#), [Other Plant Sciences Commons](#), and the [Plant Biology Commons](#)

Liu, Xiaotong; Tang, Sha; Jia, Guanqing; Schnable, James C.; Su, Haixia; Tang, Chanjuan; Zhi, Hui; and Diao, Xianmin, "The C-terminal motif of SiAGO1b is required for the regulation of growth, development and stress responses in foxtail millet (*Setaria italica* (L.) P. Beauv)" (2016). *Agronomy & Horticulture -- Faculty Publications*. 886.
<https://digitalcommons.unl.edu/agronomyfacpub/886>

This Article is brought to you for free and open access by the Agronomy and Horticulture Department at DigitalCommons@University of Nebraska - Lincoln. It has been accepted for inclusion in Agronomy & Horticulture -- Faculty Publications by an authorized administrator of DigitalCommons@University of Nebraska - Lincoln.

Authors

Xiaotong Liu, Sha Tang, Guanqing Jia, James C. Schnable, Haixia Su, Chanjuan Tang, Hui Zhi, and Xianmin Diao



RESEARCH PAPER

The C-terminal motif of SiAGO1b is required for the regulation of growth, development and stress responses in foxtail millet (*Setaria italica* (L.) P. Beauv)

Xiaotong Liu^{1,*}, Sha Tang^{1,*}, Guanqing Jia¹, James C. Schnable^{1,2}, Haixia Su¹, Chanjuan Tang¹, Hui Zhi^{1,†} and Xianmin Diao^{1,†}

¹ Institute of Crop Sciences, Chinese Academy of Agricultural Sciences, Beijing 100081, China.

² Agronomy & Horticulture, University of Nebraska-Lincoln, Beadle Center E207, Lincoln, NE 68583-0660, USA.

* These authors contributed equally to this work.

† Correspondence: zhihui@caas.cn; diaoxianmin@caas.cn

Received 15 November 2015; Accepted 7 March 2016

Editor: Greg Rebetzke, CSIRO, Plant Industries

Abstract

Foxtail millet (*Setaria italica* (L.) P. Beauv), which belongs to the Panicoideae tribe of the Poaceae, is an important grain crop widely grown in Northern China and India. It is currently developing into a novel model species for functional genomics of the Panicoideae as a result of its fully available reference genome sequence, small diploid genome ($2n=18$, ~510 Mb), short life cycle, small stature and prolific seed production. Argonaute 1 (AGO1), belonging to the argonaute (AGO) protein family, recruits small RNAs and regulates plant growth and development. Here, we characterized an AGO1 mutant (*siago1b*) in foxtail millet, which was induced by ethyl methanesulfonate treatment. The mutant exhibited pleiotropic developmental defects, including dwarfing stem, narrow and rolled leaves, smaller panicles and lower rates of seed setting. Map-based cloning analysis demonstrated that these phenotypic variations were attributed to a C–A transversion, and a 7-bp deletion in the C-terminus of the *SiAGO1b* gene in *siago1b*. Yeast two-hybrid assays and BiFC experiments revealed that the mutated region was an essential functional motif for the interaction between SiAGO1b and SiHYL1. Furthermore, 1598 differentially expressed genes were detected via RNA-seq-based comparison of *SiAGO1b* and wild-type plants, which revealed that *SiAGO1b* mutation influenced multiple biological processes, including energy metabolism, cell growth, programmed death and abiotic stress responses in foxtail millet. This study may provide a better understanding of the mechanisms by which *SiAGO1b* regulates the growth and development of crops.

Key words: AGO1, development, EMS mutant, foxtail millet, growth, HYL1, map-based cloning, RNA-seq.

Introduction

Foxtail millet (*Setaria italica* (L.) P. Beauv), which belongs to the Panicoideae subfamily, was domesticated from the wild species, green foxtail (*Setaria viridis* (L.) P. Beauv) more than 8000 years ago in Northern China (Zohary *et al.*, 2012). It remains an important cereal crop in arid and semi-arid

regions of China and India. Reference genomes of two different foxtail millet accessions are available (Bennetzen *et al.*, 2012; Zhang *et al.*, 2012). Comparative genome analysis revealed a high level of collinearity between foxtail millet and rice (*Oryza sativa*) (Devos and Gale, 1997), indicating

a promising future for comparative functional genomics. In addition, foxtail millet has been proposed recently as a novel model species for functional genomics studies of the Panicoideae because of its small diploid genome ($2n=18$, ~510Mb), short life cycle, small stature, prolific seed production and C_4 photosynthesis (Diao *et al.*, 2014; Muthamilarasan and Prasad, 2015).

RNA interference (RNAi) is a conserved mechanism that acts as both a defense mechanism against viruses and transposon blooms, and a method of gene regulation that can influence either transcription rate or mRNA stability (Baulcombe, 2004; Vaucheret, 2006). Both transcriptional and post-transcriptional RNAi mechanisms depend on short noncoding RNAs such as small interfering RNAs (siRNAs) and microRNAs (miRNAs). To date, this mechanism has been shown to regulate various biological processes including development, metabolism, and immunity in both plants and animals (Zhang *et al.*, 2013). RNAi-mediated gene silencing typically caused the destruction of specific mRNA molecules (Finnegan and Matzke, 2003). Dicer-like protein (DCL) and Argonaute (AGO) are two vital proteins in the plant RNAi process. DCL proteins contain two domains that possess endonuclease function. DCL slices mRNA into 21–25 nt small RNAs (sRNAs). The sRNAs are then captured by AGO to form the core of the RNA-induced silencing complex (RISC). The sRNAs unwind into single strands and lead the RISC to target mRNA. The RISC then captures the target mRNA and cleaves it into segments. Thus, the target genes are silenced post-transcriptionally (Baulcombe, 2004).

The AGO family contains ten members in *Arabidopsis thaliana* (Vaucheret, 2008), 19 in rice (Kapoor *et al.*, 2008) and 17 in foxtail millet (Luo *et al.*, 2013; Bennetzen *et al.*, 2012). These members can be divided into four subfamilies: MEL1, AGO4, AGO7, and AGO1. MEL1 is involved in premeiotic mitosis and meiosis during sporophyte development (Nonomura *et al.*, 2007). The AGO4 subfamily combines with siRNA to form complexes that then recruit DNA methyltransferase DOMAINS REARRANGED METHYLTRANSFERASE 2 (DRM2) and other proteins to mediate methylation modification in DNA fragments containing sequences complementary to siRNA sequences (Ye *et al.*, 2012). AGO7 participates in the *trans*-acting small interfering RNA (ta-siRNA) pathway (Nagasaki *et al.*, 2007). AGO1 is the core element of the RISC complex. AGO1 combines with 5'-U miRNAs and siRNAs (Takeda *et al.*, 2008) and slices target mRNA under the guidance of miRNAs and siRNAs (Qi *et al.*, 2005). Disruption of AGO1 function in different species generally results in phenotypes including dwarfed stems, narrow leaves, and sterile inflorescences in plants (Wu *et al.*, 2009). Previous research on *Arabidopsis* showed that AGO1 can interact with HYPONASTIC LEAVES 1 (HYL1), an important protein that plays a role in the correct recognition of slice sites in target mRNAs (Fang and Spector, 2007; Yang *et al.*, 2014). *hyl1* mutants show similar phenotypes to *ago1* mutants and exhibit greater sensitivity to abscisic acid (ABA) (Lu and Fedoroff, 2000).

The reference genome for foxtail millet included five genes belonging to the AGO1 subfamily (Bennetzen *et al.*, 2012); however, the specific functions of these genes are uncharacterized. AGO proteins contain three characteristic domains: PAZ, MID, and PIWI (Song and Joshua-Tor, 2006). The PAZ domain binds to the 3' ends of sRNAs (Mi *et al.*, 2008). The MID domain binds to the 5' ends of sRNAs (Ma *et al.*, 2005). The PIWI domain has an RNase H function that provides the mRNA slicer activity (Liu *et al.*, 2004; Rivas *et al.*, 2005; Song *et al.*, 2004). In this study, we employed a forward genetics approach to map and characterize an ethyl methane-sulfonate (EMS)-induced foxtail millet mutant that exhibited pleiotropic defects in plant growth and development, as well as hypersensitivity to ABA and drought stress. Map-based cloning identified the candidate gene as *SiAGO1b*, which encodes an argonaute protein, an important component of the RNA-induced silencing complex. The *siago1b* mutant allele identified in this study does not appear to contain any polymorphisms in these three conserved domains; however, it does encode a protein that lacks a C-terminal region of SiAGO1b. We show that this region, not previously believed to be essential for AGO1 function, influences the protein's interaction with SiHYL1, which affects growth, development and drought tolerance in foxtail millet. Transcriptome analysis revealed that the *SiAGO1b* mutation strongly influenced transcriptional regulation in foxtail millet. These results demonstrate the functional role of SiAGO1b in foxtail millet and support its importance in plant growth and development.

Materials and methods

Plant materials and growth conditions

The *siago1b* mutant was derived by EMS treatment of the foxtail millet variety Yugu1 (the accession used for the creation of the reference genome sequence). Yugu1 seeds were mutagenized with 0.5% (v/v) EMS solution overnight. One M_2 line was identified that exhibited the phenotype of dwarfing, narrow and rolled leaves, and lower seed setting rate. For morphological analysis, the mutant line was backcrossed to Yugu1 and selfed to clean the background mutations. The segregation ratio of normal and mutant phenotypes was recorded. Ten individuals of the *siago1b* mutants and wild-type plants were selected to measure the agronomic traits.

Assessment of drought tolerance and ABA response

To investigate variation in drought tolerance of the *siago1b* mutant, well-watered mutant and wild-type plants were subjected to drought treatment at either the seeding stage (6 days after germination) or four leaves stage (3 weeks after germination). Water was withheld for 12 days, and plants were then re-watered for 5 days. In addition, variation in water loss rates of fresh leaves between wild-type and *siago1b* mutant plants were monitored as described previously (Han *et al.*, 2013) for leaves excised from wild-type and *siago1b* mutant plants grown for 25 d in a culture room at 28 °C under 16/8 h light/dark cycles. Ten independent biological replicates were used for each measurement.

To assess ABA responses, foxtail millet seeds of *siago1b* and Yugu1 were germinated on moist filter paper containing 0, 2, 5 and 10 μ M concentrations of ABA. Germination rates were recorded after 10 days in the growth chamber. Fifty seeds were used for each

ABA treatment and three independent replicates were carried out for each combination of genotype and treatment. After germination, the lengths of cotyledons and roots were measured for 10 individuals from each ABA treatment.

Mapping and cloning of SiAGO1b

For map-based cloning, an F₂ mapping population derived from a cross between the *siago1b* mutant and the foxtail millet variety Liaogul was constructed and grown from June to September at the Shunyi Station of the Chinese Academy of Agricultural Sciences in Beijing, China. Liaogul is a foxtail millet cultivar that flowers at approximately the same time as Yugul but shows a high density of genetic polymorphisms relative to Yugul. Genomic DNA from F₂ plants was extracted for segregation analysis using available simple sequence repeat (SSR) markers (Zhang *et al.*, 2014). New SSR markers were developed based on the foxtail millet genome sequence information from the *S. italica* genome project V2.2 (<http://www.phytozome.net>) database if necessary. Single-nucleotide polymorphism (SNP) markers were developed based on SNP comparison data between Yugul and Liaogul (Jia *et al.*, 2013). The SSR marker primer sequences and SNP marker loci are listed in [Supplementary Table S1](#) at *JXB* online.

Sequencing and phylogenetic analysis of candidate proteins

Reference sequences of the candidate genes located in the mapping region were retrieved from the *S. italica* genome project V2.2. Genes in the mapped region were PCR amplified and the PCR products were sequenced using an Applied Biosystems 3730 sequencer (Applied Biosystems, Foster City, CA, USA) and analysed by DNAMAN8 software (Lynnon Biosoft, Quebec, Canada). Alignments of full-length candidate protein sequences used for phylogenetic analysis were produced by CLUSTALW (Thompson *et al.*, 2002). The phylogenetic tree was constructed using MEGA5.0 software (Tamura *et al.*, 2011) and the neighbor-joining method, with 1000 bootstrap value trials. The alignment file is included in [Supplementary Table S2](#).

Yeast two-hybrid analysis

A yeast two-hybrid assay was performed using the Matchmaker Gold Yeast Two-Hybrid System (Cat no. 630489, Clontech, Mountain View, CA, USA). The full-length coding regions of *SiAGO1b*/*siago1b* and *SiHYL1* were fused in frame to pGBKT7 and pGADT7, separately, to construct pGBKT7-*SiAGO1b*, pGBKT7- Δ *SiAGO1b* and pGADT7-*SiHYL1* vectors. Test vectors were co-transformed into the yeast strain Gold *Saccharomyces cerevisiae*, and interactions were tested by SD/-Ade/-His/-Leu/-Trp plate selection, following the manufacturer's instructions.

Bimolecular fluorescence complementation assay in foxtail millet protoplasts

For the bimolecular fluorescence complementation (BiFC) assay, *SiAGO1b* and Δ *SiAGO1b* were each cloned into the pSPYNE vector and fused to the N-terminus of the yellow fluorescent protein (YFP). The coding sequence of *SiHYL1* was cloned into the pSPYCE vector, resulting in a fusion open reading frame (ORF) that also contained the C-terminus of the YFP. Protoplasts were isolated from fresh leaves of 7d-old foxtail millet seedling. Both protoplast isolation and transfection followed a protocol described previously (Kim *et al.*, 2015). To investigate the expression and subcellular localization of the mutated gene, Δ *SiAGO1b* was recombined into p16318:GFP vector, and introduced into foxtail millet protoplasts by PEG-mediated transfection. YFP and green fluorescent protein (GFP) fluorescence was detected and captured by confocal microscopy (LSM700, Carl Zeiss, Germany).

Transcriptome sequencing and quantitative real-time reverse transcription PCR analysis

Mutant *siago1b* and wild-type (WT) Yugul plants were grown in a growth chamber with 16h of light at 28 °C and 8h of dark at 25 °C each day for 3 weeks. The aboveground parts of *siago1b* and WT plants were harvested and total RNA was extracted for transcriptome sequencing. RNA quality and purity were examined using an Agilent Bioanalyzer 2100 (Agilent Technologies, Waldbronn, Germany). The cDNA library was constructed following the Illumina sequencing manual. The cDNA libraries of mutant *siago1b* and the WT were sequenced on an Illumina HiSeq 2000 Genome Analyzer (Illumina, San Diego, CA, USA) with three independent biological replicates for each genotype. Raw sequencing data obtained in this study have been deposited at EMBL-EBI in the European Nucleotide Archive database under the accession number ERP014695. For the quantitative real-time reverse transcription PCR (qRT-PCR) assay, RNA was extracted from the leaves, panicles, and stems of *siago1b* and WT plants that had developed to the heading stage using Trizol (Cat no. 15596-026, Invitrogen, Paisley, UK). After removing contaminating DNAs with a Purelink RNA Kit (Cat no. 12183018, Invitrogen, UK), the RNAs were reverse transcribed using a PrimeScript II 1st Strand cDNA Synthesis Kit (Cat no. 6210A, Takara, Otsu Shiga, Japan). The cDNAs were then used as templates for qRT-PCR. Quantitative PCR was performed using a FastStart Universal SYBR Green Master kit (Cat no. 04913914001, Roche, Mannheim, Germany) on an Applied Biosystems 7300 Analyzer (Applied Biosystems, Foster City, CA, USA). The *S. italica* Actin gene (primer pairs: 5'-GTGCTTTCCTCTACGCCAGTG-3', 5'-ACCGCTGAGCACAATGTTACCA-3') was used as the internal control. The primers used for qRT-PCR are listed in [Supplementary Table S3](#). Each qRT-PCR assay was carried out with three independent replicates and each replicate corresponded to three technical repeats.

Analysis of the transcriptome data

The 100-bp paired-end reads generated from the *siago1b* and WT plants were processed by removing contaminants (reads containing adapters, unknown or low-quality bases) using in-house Perl scripts, and then trimmed using SolexaQA (Hiremath *et al.*, 2011). Clean reads were aligned to the foxtail millet genome database (*S. italica* v2.2, DOE-JGI, www.phytozome.net) using Bowtie2 and TopHat (Langdon, 2015). Differentially expressed genes (DEGs) and transcript expression analysis were performed using Cufflinks (Trapnell *et al.*, 2012). Genes with a false discovery rate ≤ 0.001 and an absolute log₂-fold change value ≥ 1 were identified as DEGs. To obtain functional annotation and classification for DEGs, we used Blast2GO to perform gene ontology (GO) annotations with regard to biological process, molecular function and cellular component (Conesa and Gotz, 2008). AgriGO was used to perform GO functional enrichment analysis with default parameters (Du *et al.*, 2010). Enriched GO terms were visualized by ReviGO (Supek *et al.*, 2011) and Cytoscape software (Shannon *et al.*, 2003). For pathway analysis, all DEGs were mapped to terms in the Kyoto Encyclopedia of Genes and Genomes (KEGG) database. KOBAS 2.0 was employed to identify statistically significantly enriched metabolic pathways (Xie *et al.*, 2011). Twenty-nine genes were selected to validate the gene expression in the Illumina data using qRT-PCR.

Results

The siago1b mutant displays pleiotropic developmental defects

At maturity, *siago1b* plants were ~70% of the height of WT plants (Fig. 1A). The *siago1b* internodes from the top to the

bottom were shorter and narrower than wild-type plants (Fig. 1B). The peduncle length, leaf length, leaf width, panicle length, and panicle diameter were diminished significantly in *siago1b* plants (Figs. 1C, D). Grain number per branch also varied between *siago1b* and wild-type plants with the WT averaging 118 grains per branch, but *siago1b* only 37 grains per branch (Fig. 2). However, no significant variation between the two was observed for the number of primary branches per panicle or 1000-grain weight (Fig. 2). These phenotypes were consistent with the *ago1b* mutant in rice (Wu *et al.*, 2009).

Drought and ABA response in seedling growth of *siago1b*

Both wild-type and *siago1b* seedlings were subjected to a 2-week drought treatment at either the emergence or four leaf stage. During water deprivation, the *siago1b* mutant plants withered and showed more severe wilting than the WT plants. WT seedlings showed obvious wilting on day 12, while the *siago1b* mutant seedlings exhibited obvious wilting by day 6 and most *siago1b* individuals were dead and desiccated by day 12 (Fig. 3). Additionally, *siago1b* seedlings lost water more quickly than WT seedlings did (Fig. 4A).

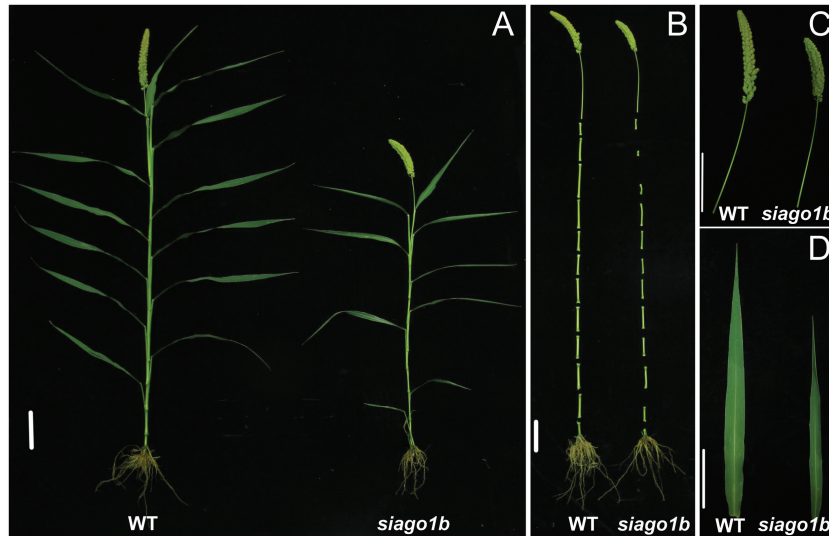


Fig. 1. The phenotypes of the wild-type (WT) and *siago1b*. (A) The gross morphologies of the WT and *siago1b*. (B) The panicles and internodes of the WT and *siago1b*. (C) The panicles and peduncles of the WT and *siago1b*. (D) The second upper leaves of the WT and *siago1b*. Scale bar: 10 cm.

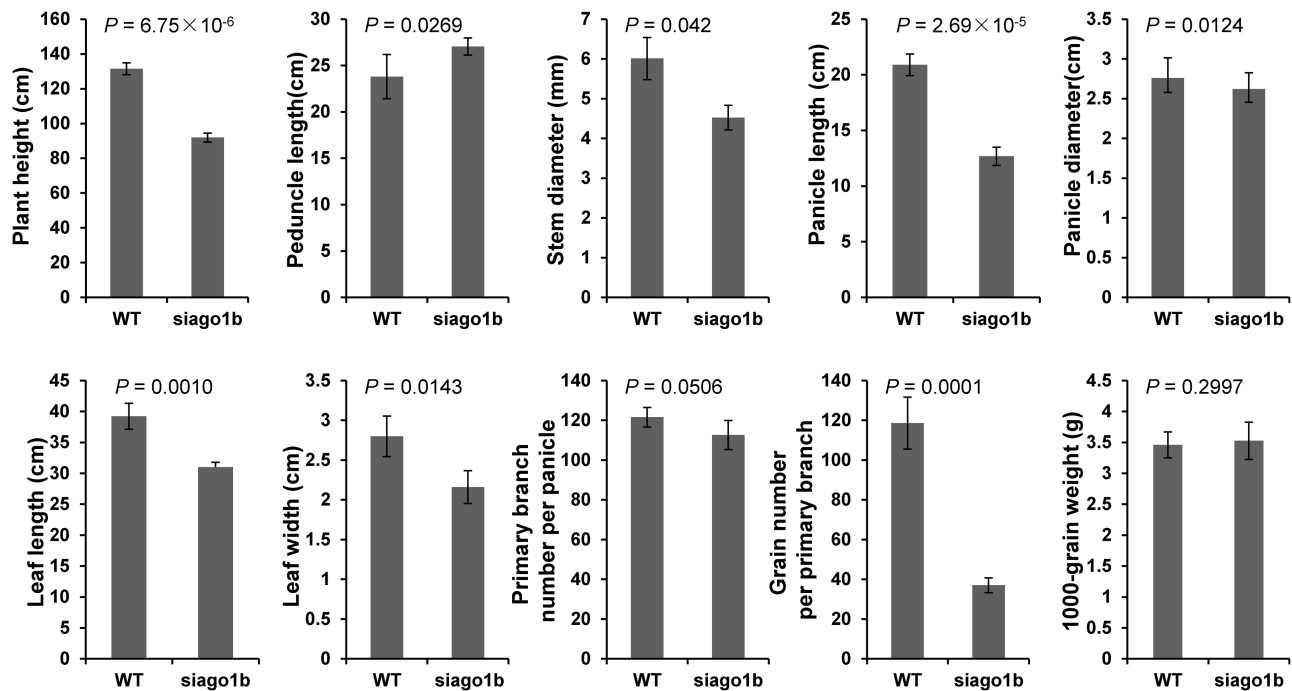


Fig. 2. Phenotype statistics of *siago1b* and the wild-type (WT). The statistics of ten *S. italica* agronomic traits of the WT and *siago1b*. Data are the means of ten independent biological replicates and the *P* value of Welch's two-sample *t* test are shown.

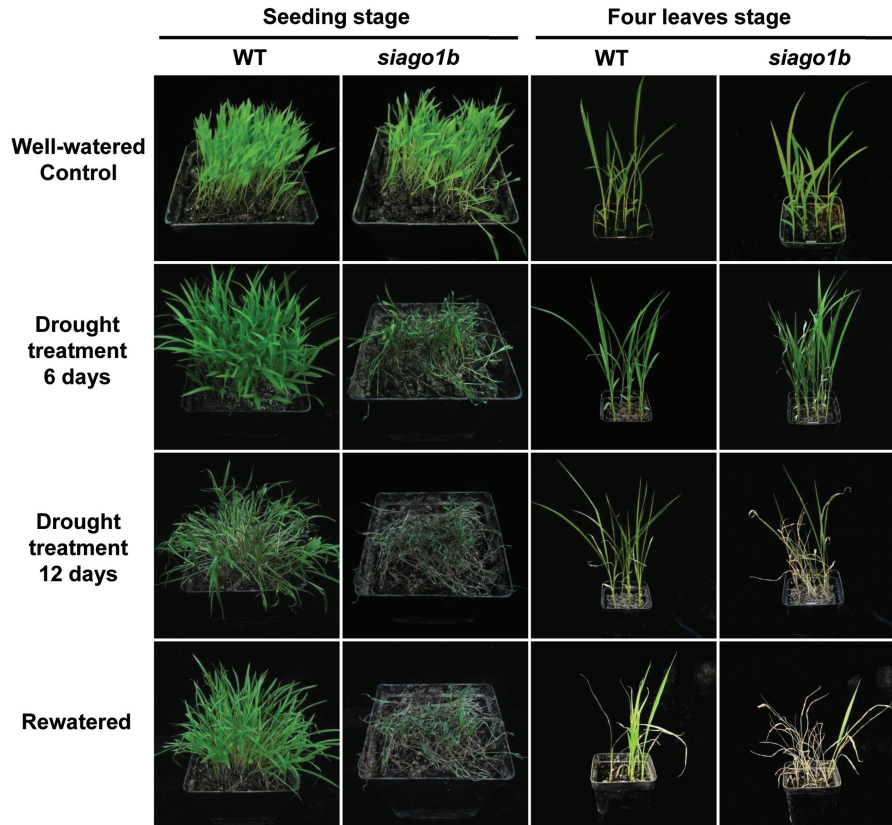


Fig. 3. Morphological differences in the drought tolerance of *siago1b* and the wild-type (WT). Seeding stage refers to plants grown in soil for 10 days after sowing under well-watered conditions. Four leaves stage refers to plants grown for 3 weeks before drought treatment. Water was withheld for 12 days, after which the plants were rewatered for 5 days.

To investigate ABA responses of the mutants, we quantified the seed germination rate (SGR) of *siago1b* and wild-type plants under different ABA concentrations. The SGR of WT was slightly affected by exogenous ABA, whereas for the *siago1b* mutant, the SGR decreased significantly in response to exogenous ABA. Under 10 μM ABA treatment, none of the mutant seeds germinated (150 seeds, 3 independent replicates, 10 days after sowing), while the SGR of WT seeds was above 70% under the same treatment conditions (Fig. 4B). Growth of *siago1b* mutant seedlings was also severely affected by exogenous ABA treatment, as evidenced by shorter primary root and cotyledon (Fig. 4C, D, Supplementary Fig. S1) than WT plants when treated with equal concentrations of exogenous ABA.

Map-based cloning of the SiAGO1b gene

The *SiAGO1b* gene was isolated using a map-based cloning approach and an F_2 population derived from a cross of mutant *siago1b* and wild-type foxtail millet plants of the variety Liaogu1. In the F_2 generation, a total 780 individuals were phenotypically scored, of which 595 were wild-type and 185 exhibited a dwarf phenotype, with narrow and rolled leaves, which was consistent with a mendelian ratio of 3:1 for normal phenotype to mutant phenotype offspring ($\chi^2=0.62 < \chi^2_{0.05}=3.84$). This suggested that a single recessive gene controlled the multiple phenotypes observed for *siago1b*. For map-based cloning, more than 800 F_2 homozygous recessive individuals were used. Bulk segregation analysis showed that the *SiAGO1b* gene was on chromosome 7

and was genetically linked with SSR markers CAAS7027 and CAAS7029. Additional SSR and SNP markers were employed to fine-map *SiAGO1b* to a 46.3-kb region between SNP markers SNP027326466 and SNP27372797 on chromosome 7, with two and four recombinants, respectively (Fig. 5).

SiAGO1b encodes an argonaute protein

Using the *S. italica* genome database V2.2, five ORFs were identified in the mapping interval (Table 1). Sequencing of genomic DNA from the target region revealed a 7-bp deletion and a 1-bp shift in the 22nd exon of *Seita.7G201100* (Fig. 6A). *Seita.7G201100* encodes a protein containing the two characteristic domains of argonaute (AGO) proteins: PAZ and PIWI (Fig. 6B). Phylogenetic analysis and protein sequence alignment showed that the *Seita.7G201100* was most closely related to OsAGO1b, which belongs to subfamily AGO1 (Fig. 6C). Therefore, the target gene was named *SiAGO1b*. The *siago1b* mutant allele was predicted to encode a protein ($\Delta\text{SiAGO1b}$) with a frame shift mutation after amino acid 1068 and early termination at amino acid 1073 (Fig. 6B). Multiple sequence alignment of the SiAGO1b protein and its homologous proteins in soybean (*Glycine max*), maize (*Zea mays*), rice, *Brachypodium distachyon* and wheat (*Triticum aestivum*) revealed that the C-terminal motif of the SiAGO1b (–PLPALKENVKRVMFYC) protein is highly conserved among these organisms. However, ΔSiAGO1 has a mutation in this region (–QLSRRRT) (Fig. 6D). The alignment result indicated that the mutated region of SiAGO1b protein is probably a functional motif.

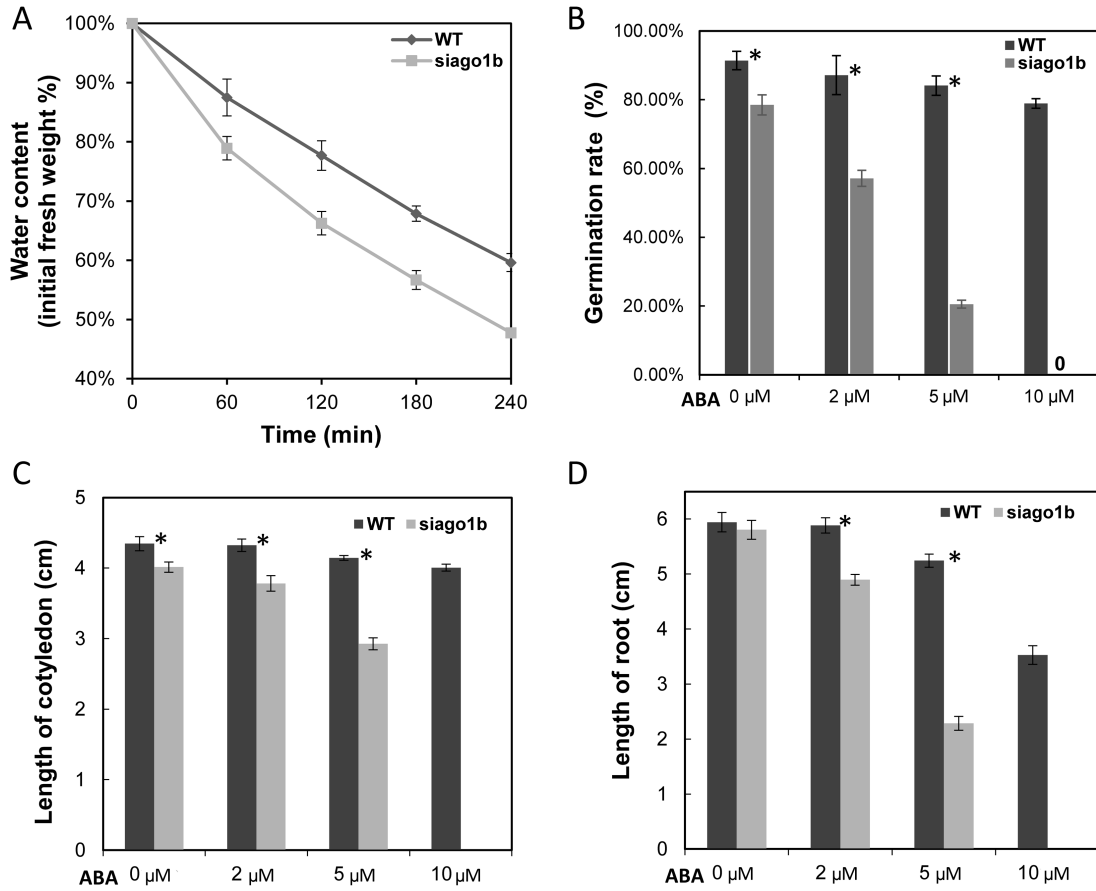


Fig. 4. *Siago1b* mutant response to dehydration and ABA treatment. (A) Water loss from whole seedling of *siago1b* mutant and the WT. Water loss is expressed as the percentage of initial fresh weight of seedlings. (B, C, D) Difference in germination rates, cotyledon length, and primary root length between *siago1b* mutant and the WT in response to exogenous ABA. Data are means from ten individuals. Asterisks indicate a significant difference between *siago1b* and WT plants ($n=10$, Welch's two-sample t test, $P<0.001$).

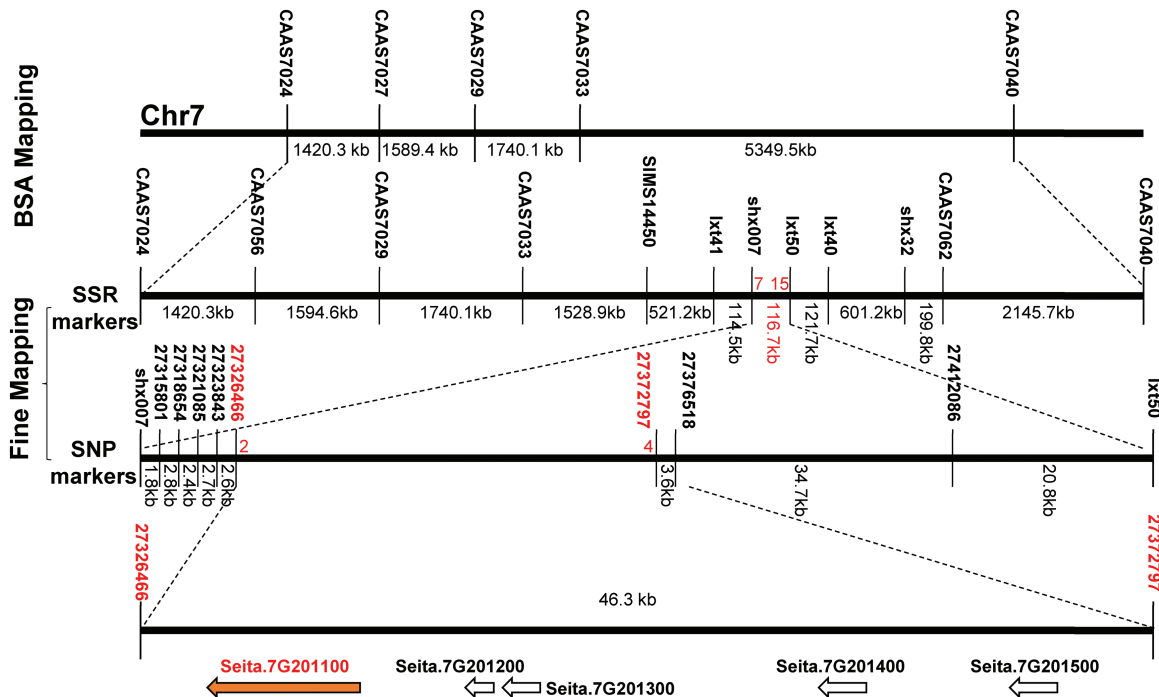


Fig. 5. Map-based cloning of the *SiAGO1b* gene. *SiAGO1b* was mapped in the interval between molecular markers SNP027326466 and SNP 27372797 on chromosome 7 using 780 recessive individual plants showing a mutant-like phenotype from an F_2 population. Numbers under the markers indicate recombinants. Numbers between markers indicate the physical distance. The white arrows indicate ORFs. The orange arrow stands for the candidate gene.

SiAGO1b mutation influenced its interaction with *SiHYL1* and transcript accumulation level in leaf and panicle

The Arabidopsis homologous protein of *SiAGO1b*, *AtAGO1*, interacts with the *HYL1* protein (Fang and Spector, 2007). In foxtail millet, *Seita.7G329000* is the homolog of *HYL1*, which was named *SiHYL1*. The yeast strain (Gold *Saccharomyces cerevisiae*) carrying BD-*SiAGO1b*+AD-*SiHYL1* grew well on SD/-Ade/-His/-Leu/-Trp yeast growth medium. However, the yeast strain carrying BD- Δ *SiAGO1b*+AD-*SiHYL1* could not grow on SD/-Ade/-His/-Leu/-Trp yeast growth medium (Fig. 7A).

To further confirm the interaction between *SiAGO1b* (Δ *SiAGO1b*) and *SiHYL1*, we employed BiFC assays with *SiAGO1b* tagged with the N-terminal domain of YFP and

Table 1. Gene IDs, locations and functional annotations in the mapped region

Gene ID	Location	Functional annotation
<i>Seita.7G201100</i>	scaffold_7: 27330567 - 27344429	Eukaryotic translation initiation factor 2C
<i>Seita.7G201200</i>	scaffold_7: 27338776 - 27340117	There are no functional annotations for this locus
<i>Seita.7G201300</i>	scaffold_7: 27340287- 27342020	There are no functional annotations for this locus
<i>Seita.7G201400</i>	scaffold_7: 27354369 - 27356190	Eukaryotic translation initiation factor 3
<i>Seita.7G201500</i>	scaffold_7: 27365483 - 27367466	Protein of unknown function (DUF1618)

SiHYL1 fused into the C-terminal domain of YFP. A YFP fluorescence signal was detected in the nucleus, indicating that *SiAGO1b* interacts with *SiHYL1* (Fig. 7B, Supplementary Fig. S2). The result is consistent with a previous report from Arabidopsis (Fang and Spector, 2007). However, no BiFC signal was detected between the mutated protein Δ *SiAGO1b* and *SiHYL1*. Simultaneously, we determined the subcellular localization of Δ *SiAGO1b*. A fluorescence signal from a Δ *SiAGO1b*-GFP fusion protein can be clearly detected in the nucleus, indicating that loss of C-terminal motif in *SiAGO1b* does not affect its translation or subcellular localization (see Supplementary Fig. S3). Together, these results suggest that the C-terminal polypeptide of *SiAGO1b* is necessary for protein-protein interaction between *SiAGO1b* and *SiHYL1*.

qRT-PCR was used to assess the expression of *SiAGO1b* in different tissues. The relative expression level of *SiAGO1b* was higher in *siago1b* mutant panicles and leaves than wild-type, but expression in the stem was not significantly different between the two genotypes (Fig. 7C). This suggests that there may be a feedback mechanism to increase the expression of *SiAGO1b* in *siago1b* mutant panicles and leaves in response to the loss of the functional *SiAGO1b* protein activity.

DEG analysis of *siago1b* mutant by transcriptome sequencing

Argonaute protein is a key component of the RISC complex that regulates gene expression in a range of biological processes (Mallory and Hervé, 2010). Therefore, mutations of *AGO1* are

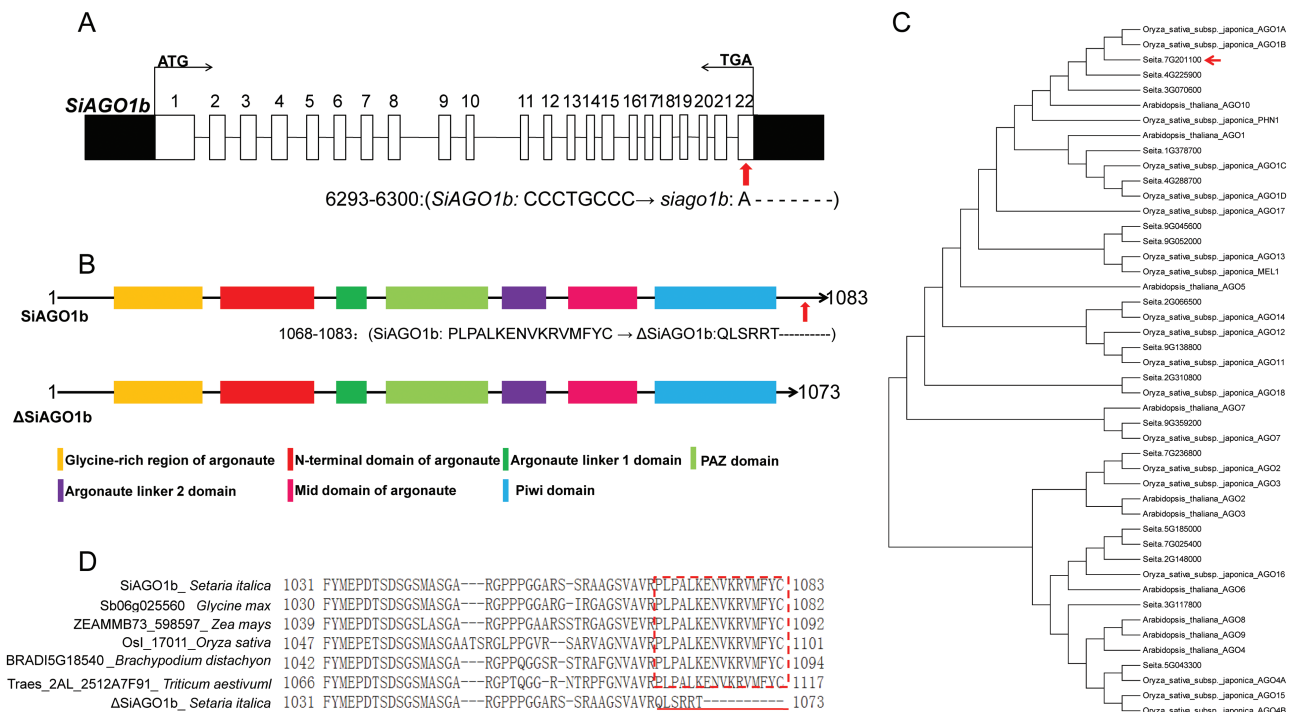


Fig. 6. The structure and phylogenetic analysis of target gene *SiAGO1b*. (A) Gene structure of *SiAGO1b*. The mutation site is indicated by a red arrow. (B) Protein structure of the wild-type (WT) *SiAGO1b* and mutant Δ *SiAGO1b*. The mutant site is indicated by a red arrow in WT *SiAGO1b*. (C) Phylogenetic relationships of AGO family proteins of foxtail millet, Arabidopsis and rice. *SiAGO1b* was most closely related to *OsAGO1*, which belongs to subfamily AGO1. A red arrow indicates the position of *SiAGO1b*. (D) The multiple alignments of *SiAGO1b* homologous proteins in different organisms. The organism name and gene locus name are shown before protein sequences. Δ *SiAGO1* indicates the mutant protein. A red box indicates the C-terminal conserved region. A red line indicates the mutant protein sequence in the *siago1b* mutant.

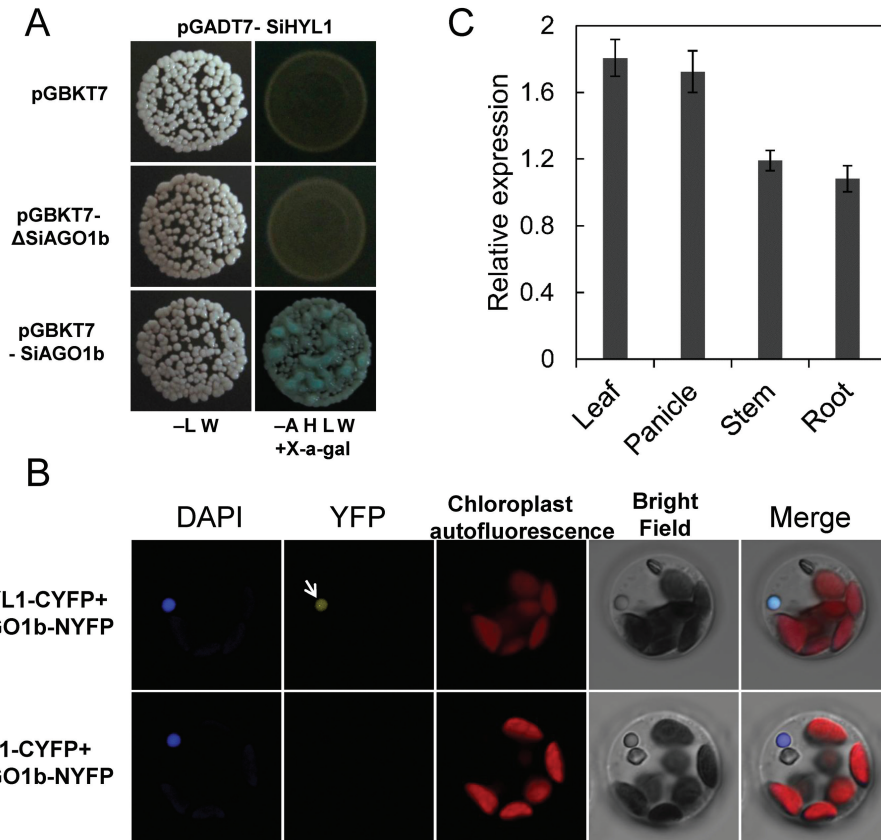


Fig. 7. The protein interaction and gene expression analysis of *SiAGO1b*. (A) Result of yeast two-hybrid assay. Yeast two-hybrid assays showing that SiHYL1 interacts with SiAGO1b, but not with mutant protein Δ SiAGO1b. –LW indicates yeast medium SD/–Leu/–Trp, –AHLW indicates yeast medium SD/–Ade/–His/–Leu/–Trp. 5-Bromo-4-chloro-3-indolyl α -D-galactopyranoside (X- α -gal) was added to the solid yeast medium, and the same amount of yeast was used in each assay. The interaction was judged from the blue color and yeast growth density. (B) The relative expression of Δ SiAGO1b gene in mutant leaf, panicle, stem, and root. Total RNA was isolated from various tissues of WT and *siago1* seedlings grown in culture. qPCR was conducted with three biological replicates. (C) BIFC experiments between SiAGO1b, mutant protein Δ SiAGO1b and SiHYL1. Protein partners was fused to an N-terminal fragment or C-terminal fragment of YFP, respectively, and co-infiltrated into foxtail millet protoplasts. DAPI was used to label the nucleus. BIFC signals between SiAGO1b and SiHYL1 were observed in nucleus region. No BIFC signals were observed between mutant protein Δ SiAGO1b and SiHYL1. Negative and positive control test is shown in [Supplementary Figs S2 and S3](#).

likely to produce both direct and indirect changes in the abundance of the downstream target genes. Transcriptome sequencing was employed to compare the expression profiles of WT and *siago1b* mutant plants, resulting in the identification of 1598 differentially expressed genes (see [Supplementary Table S4](#)). GO enrichment analysis for the up- and down-regulated genes in *siago1b* was performed to identify the major biological processes and molecular functions regulated by SiAGO1b. Thirty-nine biological processes ($P < 0.05$, [Supplementary Table S5](#)) were enriched among genes up-regulated in *siago1b*, and 22 for the down-regulated genes ($P < 0.05$, [Supplementary Table S6](#)). GO terms involved in stress responses and oxidation–reduction were enriched among both up- and down-regulated genes. Interestingly, the majority of all genes annotated as participated in transcriptional regulation, protein metabolism, and programmed cell death were up-regulated in the mutant ([Fig. 8A](#)). GO terms associated with energy metabolism (e.g. carbohydrate metabolism and lipid metabolism) were enriched specifically among the genes down-regulated in *siago1b* ([Fig. 8B](#)). [Supplementary Fig. S4](#) shows the DEGs distributed among the seven most enriched biological and 15 molecular GO terms. [Supplementary Table S7](#) lists the 37 up-regulated genes and 34 down-regulated genes, which showed the greatest change in expression between mutant and

wild-type plants. These genes were mainly distributed in three functional pathways: genes related to abscisic acid (ABA) signaling and stress responses, transcription factors controlling organ development, and genes regulating floral development ([Fig. 8C](#)). Other genes controlling plant normal growth and development showed significant changes in expression. Notably, two DEGs had no homologous genes in Arabidopsis and rice. These may be foxtail millet-specific genes that possess unique functions ([Supplementary Table S8](#)). Among these 71 genes with the greatest difference in expression between mutant and wild-type plants, 27 had homologs in Arabidopsis that have already been annotated ([Table 2](#)). These 29 genes were selected to validate the RNA-seq gene expression analysis through the use of qRT-PCR ([Supplementary Fig. S5](#)).

Discussion

The C-terminus of SiAGO1b is an essential motif for the interaction between SiAGO1b and SiHYL1, which plays an important role in plant growth and development

To maintain normal growth and development, plant gene expression must be under strict control. AGO proteins mediate target cleavage under the guidance of sRNAs, such as

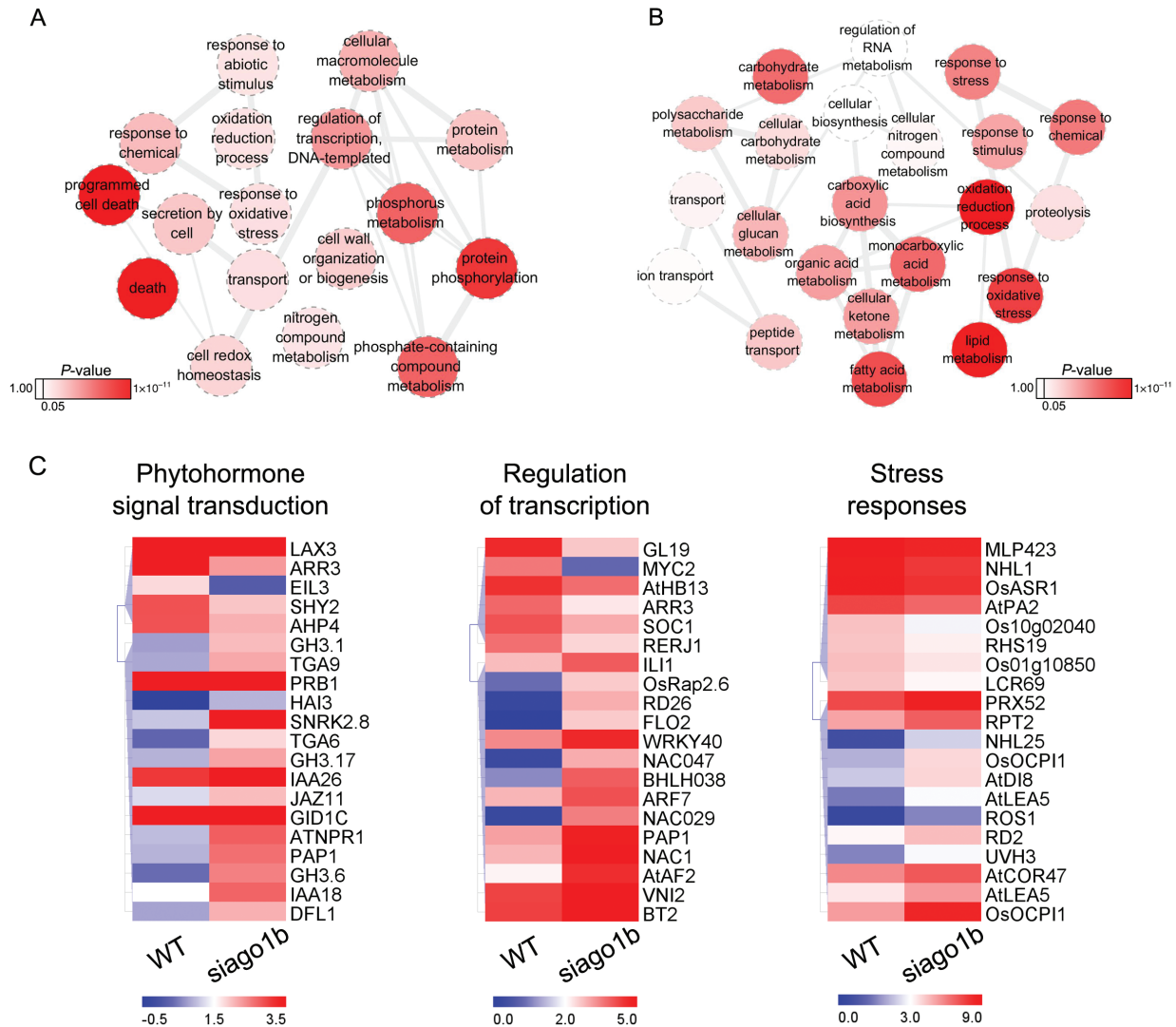


Fig. 8. Enriched biological processes and candidate differentially expressed genes (DEGs) of the *siago1b* mutant. (A, B) Functional enrichment analysis of up- and down-regulated genes. Each circle represent a gene ontology (GO) term in red, as shown in the color bar ranging from 1.0 to 1×10^{-11} (P value); $P < 0.05$ was used as the threshold. (C) Expression patterns of DEGs previously characterized in Arabidopsis or rice. Clustering based on average \log_2 FPKM of genes involved in phytohormone signal transduction, transcription regulation and stress responses.

miRNAs. Most miRNAs are incorporated into AGO1-associated silencing complexes in plants. AGO1 is considered the most important slicer protein for sRNA-mediated target-RNA cleavage (Voinnet, 2009). *AtAGO1* was the first reported member of the *AGO* gene family, so named because the leaves of the *atago1* mutant showed an *Argonauta* squid tentacles-like character (Bohmer et al., 1998). Rice has four *AGO1* homologs. Rice *AGO1* homolog knockdown mutants showed pleiotropic developmental phenotypes. The rice *AGO1* mutants exhibited severe dwarfing, narrow and rolled leaves, and a lower seed setting rate (Wu et al., 2009). The foxtail millet *siago1b* mutant showed many of the same phenotypes observed in rice. In addition, the peduncle length, panicle length and panicle diameter were diminished significantly in the *siago1b* mutant. The *HYL1* protein was previously shown to interact with AGO1 in Arabidopsis (Fang and Spector, 2007). Like the *ago1* mutant, the *hyl1* mutant exhibited dwarf, narrow and rolled leaves and a lower seed setting rate. Two ABA-inducible genes, *KIN2* and *COR47* (Gilmour

et al., 1992; Kurkela and Borg-Franck, 1992), exhibited increased transcript levels in the *hyl1* mutant. This suggested that the *HYL1* is sensitive to ABA (Lu and Fedoroff, 2000).

Sequencing of the *siago1b* allele did not identify any mutations in the characteristic domains of AGO1 protein: PAZ, MID and PIWI (Song and Joshua-Tor, 2006). However, a 7-bp deletion and 1-bp shift were identified in the last exon of *SiAGO1b*. To investigate whether the mutated region is a functional element in foxtail millet, the foxtail millet homolog of *HYL1* (*SiHYL1*) was cloned. Yeast two-hybrid assays and BiFC experiments revealed that WT *SiAGO1b* protein interacts with *SiHYL1* protein but the mutant *SiAGO1b* protein does not (Fig. 7A, 7B). Thus, the C-terminus of *SiAGO1* is essential for its interaction with *SiHYL*. The *SiAGO1* C-terminus has a highly conserved motif across different plant species (Fig. 6D). The *siago1b* mutant lacks this motif, which may result in a structural alteration that abolishes the ability to interact with *SiHYL1*. The loss of function in the C-terminus of *SiAGO1b* made the mutant more sensitive to

Table 2. Twenty-seven genes whose expression was significantly altered between the wild-type and the *siago1b* mutant that have homologous genes studied in *Arabidopsis*

Gene ID	Homologous gene in <i>Arabidopsis</i>	Fold change in <i>siago1b</i>	Gene name in <i>Arabidopsis</i>	Gene annotation
<i>Seita.1G334700</i>	<i>AT1G77760.1</i>	5.711	GNR1, NIA1, NR1	Nitrate reductase 1
<i>Seita.9G440900</i>	<i>AT5G65010.1</i>	5.205	ASN2	Asparagine synthetase 2
<i>Seita.6G178500</i>	<i>AT1G77760.1</i>	3.957	GNR1, NIA1, NR1	Nitrate reductase 1
<i>Seita.7G150500</i>	<i>AT3G54420.1</i>	3.492	ATCHITIV, ATEP3, CHIV, EP3	Homolog of carrot EP3-3 chitinase
<i>Seita.8G132600</i>	<i>AT3G48280.1</i>	3.237	CYP71A25	Cytochrome P450, family 71, subfamily A, polypeptide 25
<i>Seita.2G270400</i>	<i>AT1G02850.2</i>	3.141	BGLU11	β -Glucosidase 11
<i>Seita.8G008100</i>	<i>AT1G69490.1</i>	3.067	ANAC029, ATNAP, NAP	NAC-like, activated by AP3/PI
<i>Seita.9G379000</i>	<i>AT1G78290.2</i>	2.800	SNRK2-8, SNRK2.8, SRK2C	Protein kinase superfamily protein
<i>Seita.5G455700</i>	<i>AT3G56970.1</i>	2.709	BHLH038, ORG2	Basic helix-loop-helix (bHLH)
<i>Seita.2G368800</i>	<i>AT3G18830.1</i>	2.427	ATPLT5, ATPMT5, PMT5	DNA-binding superfamily protein
<i>Seita.3G386200</i>	<i>AT1G56010.2</i>	2.305	anac021, ANAC022, NAC1	Polyol/monosaccharide transporter 5
<i>Seita.7G059700</i>	<i>AT5G45890.1</i>	-11.917	SAG12	NAC domain containing protein 1
<i>Seita.6G048800</i>	<i>AT5G23960.1</i>	-4.917	ATTPS21, TPS21	Senescence-associated gene 12
<i>Seita.9G011100</i>	<i>AT3G26300.1</i>	-4.516	CYP71B34	Terpene synthase 21
<i>Seita.8G200200</i>	<i>AT3G07990.1</i>	-3.120	SCPL27	Cytochrome P450, family 71, subfamily B, polypeptide 34
<i>Seita.8G247500</i>	<i>AT4G37050.1</i>	-2.916	AtPLAIVC, PLA V, PLP4	Serine carboxypeptidase-like 27
<i>Seita.6G233600</i>	<i>AT1G32640.1</i>	-2.804	ATMYC2, JAI1, JIN1, MYC2, RD22BP1, ZBF1	PATATIN-like protein 4
<i>Seita.5G311800</i>	<i>AT2G19770.1</i>	-2.463	PRF5	Basic helix-loop-helix (bHLH)
<i>Seita.3G067200</i>	<i>AT5G23960.1</i>	-2.446	ATTPS21, TPS21	DNA-binding family protein
<i>Seita.1G332100</i>	<i>AT5G08640.1</i>	-2.228	ATFLS1, FLS, FLS1	Profilin 5
<i>Seita.2G134400</i>	<i>AT1G19670.1</i>	-2.214	ATCLH1,ATHCOR1,CLH1,CORI1	Terpene synthase 21
<i>Seita.1G207000</i>	<i>AT2G02860.1</i>	-2.201	ATSUC3,ATSUT2,SUC3,SUT2	Flavonol synthase 1
<i>Seita.9G471200</i>	<i>AT2G21140.1</i>	-2.171	ATPRP2,PRP2	Chlorophyllase 1
<i>Seita.8G139500</i>	<i>AT5G13930.1</i>	-2.157	ATCHS,CHS,TT4	Sucrose transporter 2
<i>Seita.5G469800</i>	<i>AT4G01470.1</i>	-1.948	ATTIP1.3,GAMMA-TIP3,TIP1;3	Proline-rich protein 2
<i>Seita.8G211600</i>	<i>AT3G09220.1</i>	-1.946	LAC7	Chalcone and stilbene synthase family protein
<i>Seita.8G212000</i>	<i>AT3G09220.1</i>	-1.910	LAC7	Tonoplast intrinsic protein 1;3
				Laccase 7
				Laccase 7

ABA and drought stress, and in addition led to the serious growth and developmental phenotypes.

The siago1b mutants are more sensitive to ABA and drought stress

Through expression analysis of the 27 genes whose homologs have already been studied in *Arabidopsis* with the most significant changes in expression in the *siago1b* mutant, several genes related to stress and abscisic acid (ABA) signal response were identified whose expressions changed markedly in *siago1b*. *GNR1* (AT1G77760.1), which was up-regulated in the mutant, encodes a cytosolic minor isoform of nitrate reductase, which is involved in the first step of nitrate assimilation and contributes about 15% of the nitrate reductase activity in shoots. The stomata of the mutant are less sensitive to ABA, and the mutant plants exhibit very poor growth on nitrate medium (Desikan et al., 2002). The up-regulated gene *SNRK2-8* (AT1G78290.2)

encodes a member of the SNF1-related protein kinase (SnRK2) family. *SNRK2-8* plays an important role in the ABA pathway, osmotic stress and drought stress signaling in *Arabidopsis* (Mizoguchi et al., 2010). Up-regulated gene *ATCHITIV* (AT3G54420.1) encodes an EP3 chitinase. The expression of *ATCHITIV* responds to environmental stresses in *Arabidopsis*. For instance, *ATCHITIV* responds to cold, light intensity, wounding, salt stress, and water deprivation (Takenaka et al., 2009). The down-regulated gene *AtPLAIVC* (AT4G37050.1) encodes a patatin-related phospholipase A. *AtPLAIVC* is expressed in the gynoecium and is induced by ABA or phosphate deficiency in *Arabidopsis* roots. A loss-of-function mutant exhibited an impaired response to phosphate deficiency during root development. In addition, a novel function of *AtPLAIVC* was reported: in root development it has a function at the interface between phosphate deficiency and auxin signaling (Rietz et al., 2010). The down-regulated gene *AtFLS1* (AT1G32640.1) encodes an MYC-related transcriptional

activator with a DNA-binding domain (a basic helix–loop–helix leucine zipper motif). The transcription of this gene is induced by dehydration stress and ABA treatment (Carvalhois *et al.*, 2015). *AtSUC3* (AT2G02860.1) encodes a sucrose transporter in sieve elements and some sink tissues, and is also down-regulated in the mutant. The loss-of-function mutant of *AtSUC3* reduced the expression of genes *AtSUC2* and *AtSUC4*, which respond to abiotic stresses and ABA. Thus, *AtSUC3* is an important regulator in plant abiotic stress tolerance via the ABA signal pathway (Gong *et al.*, 2015).

A genome-wide identification and functional characterization of the argonaute gene family in foxtail millet was performed by Yadav *et al.* (2015). The study found that *SiAGO1b* had highest mRNA accumulation in all tissues compared with other AGO family members. They also reported that members of the *S. italica* AGO1 subfamily showed substantial inductions of expression in response to ABA (12.4-fold up-regulation at 1 h ABA treatment). In our study, the germination rate and seedling growth of *siago1b* were significantly repressed by exogenous ABA (Fig. 4, Supplementary Fig. S1). The seedlings of *siago1b* lost water more quickly than those of the WT. In addition, the drought tolerance ability of the *siago1b* mutant decreased obviously. It is probable that these phenomena were caused by disordered expression of ABA-related genes in the *siago1b* mutant.

The mutation of *siago1b* affected genes related to plant growth and development

The same analysis of genes with the greatest changes in expression in *siago1b* and homologs studied in Arabidopsis also identified several transcription factors. *ANAC029* (AT1G69490.1), up-regulated, encodes a NAC transcription factor. *ANAC029* plays an important role in leaf senescence in Arabidopsis and other plant species (Guo and Gan, 2006). *ANAC029* also plays a role in petal senescence, independent of endogenous ethylene control (Shinozaki *et al.*, 2014). Up-regulated gene *BHLH038* (AT3G56970.1) encodes a member of the basic helix–loop–helix transcription factor protein family. These transcription factor genes are up-regulated strongly from cell proliferation to expansion in young developing leaves of Arabidopsis. The mutant plants developed smaller rosettes than WT plants (Andriankaja *et al.*, 2014). Up-regulated gene *ANAC022* (AT1G56010) encodes a transcription factor involved in the formation of the shoot apical meristem and auxin-mediated lateral roots. The results of previous studies indicated that *ANAC022* responds to plant hormones. *ANAC022* might be involved in auxin and gibberellin signaling pathways in promoting the development of lateral roots (Wang *et al.*, 2006). These transcription factors were all up-regulated and are involved in the regulation of development and senescence of flowers, leaves, and roots. The expression changes of these transcription factors could lead to pleiotropic developmental defects in plants. The blocked growth and development phenotypes of the *siago1b* mutant were likely caused by the expression changes of these transcription factors.

Genes controlling the reproductive process were severely repressed

One of the notable phenotypes associated with the *siago1b* mutant was its significant decrease in grain yield without a decrease in thousand-grain weight. This indicated that the development process of flowers was likely defective in the *siago1b* mutant. There were DEGs whose homologs in Arabidopsis control flowering development. In addition to *ANAC029*, which plays a role in petal senescence, *AtTPS21* (AT5G23960.1), down-regulated in *siago1b*, encodes a sesquiterpene synthase involved in generating group A sesquiterpenes. The flowering stage is controlled by the expression of *AtTPS21* in Arabidopsis (Yu *et al.*, 2015). The down-regulated gene *PRF5* (AT2G19770.1) encodes a profilin 5 protein, which is an actin monomer-binding protein that regulates actin cytoskeleton organization. It is expressed predominantly in mature pollen and growing pollen tubes (Wang *et al.*, 2008). *AtTIP1.3* (AT4G01470.1), down-regulated, encodes a tonoplast intrinsic protein, belonging to a subfamily of aquaporins. It functions as a water and urea channel in pollen and contributes to normal male fertility in adverse environmental conditions (Wudick *et al.*, 2014). In addition, two genes associated with the formation of flavonoids in mutant *siago1b* were significantly down-regulated. Flavonols are important compounds for conditional male fertility in plants. *AtFLS1* (AT5G08640.1) encodes a flavonol synthase that catalyses the formation of flavonols from dihydroflavonols (Falcone *et al.*, 2010). *AtCHS* (AT5G13930.1) encodes chalcone synthase (CHS), which also plays an essential role in the biosynthesis of flavonoid (Sun *et al.*, 2015). The defective development of *siago1b* flowers may result from the repression of certain genes controlling the reproductive process.

The expression of other genes controlling plant normal growth and development was also significantly altered. For example, *ASN2* (AT5G65010.1) encodes an asparagine synthetase and was up-regulated. Mutations disrupting the function of this gene exhibit defects in development. This gene is essential for nitrogen assimilation, distribution, and remobilization in plants (Gaufichon *et al.*, 2013).

In summary, map-based cloning of an EMS-induced pleiotropic mutant in foxtail millet identified the causal gene *SiAGO1b*. Initial characterization of the mutant was carried out at the molecular level. Protein interaction and RNA-seq analysis provided some clues to the function and pathways of *SiAGO1b* in foxtail millet. These results revealed that a motif in the C-terminus of *SiAGO1b* is vitally important to maintain normal growth and drought stress tolerance. The findings of this study may help to promote further studies of how the molecular mechanism of *AGO1* is either varied or conserved among different plant species.

Supplementary data

Supplementary data are available at *JXB* online.

- Figure S1. Morphological differences in the ABA treatment.
- Figure S2. Negative control of BiFC assays.
- Figure S3. Subcellular localization of Δ SiAGO1b.

Figure S4. Differentially expressed gene (DEG) distribution in the most enriched gene ontology (GO) terms.

Figure S5. Twenty-nine differentially expressed genes (DEGs) selected for validation of the Illumina data using quantitative real-time reverse transcription PCR (qRT-PCR).

Table S1. Simple sequence repeat (SSR) primer sequences and single-nucleotide polymorphism (SNP) loci.

Table S2. Multiple sequence alignment for phylogenetic analysis.

Table S3. Primers used for qRT-PCR.

Table S4. Genes that were differentially expressed in *siago1b* compared with the wild-type.

Table S5. Thirty-nine biological processes that were enriched for the up-regulated genes.

Table S6. Twenty-two biological processes that were enriched for the down-regulated genes.

Table S7. The top 37 up-regulated genes and 34 down-regulated genes that were most differentially expressed.

Table S8. Significant differentially expressed genes between wild-type and *siago1b* mutant which have no homologous genes in *Arabidopsis* and rice.

Acknowledgements

This work was supported by the National High Technology Research and Development Program of China (863 Program) (grant number 2013AA102603), National Natural Science Foundation of China (grant numbers 31301328, 31522040), Beijing Natural Science Foundation (6142019), Fundamental Research Funds of ICS-CAAS (Grant to G.J., 2013007), China Agricultural Research System (grant number CARS07-13.5-A02), and The Agricultural Science and Technology Innovation Program of CAAS.

References

- Andriankaja ME, Danisman S, Mignolet-Spruyt LF, et al.** 2014. Transcriptional coordination between leaf cell differentiation and chloroplast development established by TCP20 and the subgroup 1b bHLH transcription factors. *Plant Molecular Biology* **85**, 233–245.
- Baulcombe D.** 2004. RNA silencing in plants. *Nature* **431**, 356–363.
- Bennetzen JL, Schmutz J, Wang H, et al.** 2012. Reference genome sequence of the model plant *Setaria*. *Nature Biotechnology* **30**, 555–561.
- Bohmer K, Camus I, Bellini C, Bouchez D, Caboche M, Benning C.** 1998. AGO1 defines a novel locus of *Arabidopsis* controlling leaf development. *EMBO Journal* **17**, 170–180.
- Carvalho LC, Dennis PG, Badri DV, Kidd BN, Vivanco JM, Schenk PM.** 2015. Linking jasmonic acid signaling, root exudates, and rhizosphere microbiomes. *Molecular Plant-Microbe Interactions* **28**, 1049–1058.
- Conesa A, Gotz S.** 2008. Blast2GO: A comprehensive suite for functional analysis in plant genomics. *International Journal of Plant Genomics* **2008**, 619832.
- Desikan R, Griffiths R, Hancock J, Neill S.** 2002. A new role for an old enzyme: nitrate reductase-mediated nitric oxide generation is required for abscisic acid-induced stomatal closure in *Arabidopsis thaliana*. *Proceedings of the National Academy of Sciences of the United States of America* **99**, 16314–16318.
- Devos KM, Gale MD.** 1997. Comparative genetics in the grasses. *Plant Molecular Biology* **35**, 3–15.
- Diao X, Schnable J, Bennetzen JL, et al.** 2014. Initiation of *Setaria* as a model plant. *Frontiers of Agricultural Science and Engineering* **1**, 16–20.
- Du Z, Zhou X, Ling Y, Zhang Z, Su Z.** 2010. agriGO: a GO analysis toolkit for the agricultural community. *Nucleic Acids Research* **38**, W64–W70.
- Falcone FM, Rius S, Emiliani J, Pourcel L, Feller A, Morohashi K, Casati P, Grotewold E.** 2010. Cloning and characterization of a UV-B-inducible maize flavonol synthase. *The Plant Journal* **62**, 77–91.
- Fang Y, Spector DL.** 2007. Identification of nuclear dicing bodies containing proteins for microRNA biogenesis in living *Arabidopsis* plants. *Current Biology* **17**, 818–823.
- Finnegan EJ, Matzke MA.** 2003. The small RNA world. *Journal of Cell Science* **116**, 4689–4693.
- Gaufichon L, Masclaux-Daubresse C, Tcherkez G, et al.** 2013. *Arabidopsis thaliana* ASN2 encoding asparagine synthetase is involved in the control of nitrogen assimilation and export during vegetative growth. *Plant, Cell & Environment* **36**, 328–342.
- Gilmour SJ, Artus NN, Thomashow MF.** 1992. cDNA sequence analysis and expression of two cold-regulated genes of *Arabidopsis thaliana*. *Plant Molecular Biology* **18**, 13–21.
- Gong X, Liu M, Zhang L, Ruan Y, Ding R, Ji Y, Zhang N, Zhang S, Farmer J, Wang C.** 2015. *Arabidopsis* AtSUC2 and AtSUC4, encoding sucrose transporters, are required for abiotic stress tolerance in an ABA-dependent pathway. *Physiologia Plantarum* **153**, 119–136.
- Guo Y, Gan S.** 2006. AtNAP, a NAC family transcription factor, has an important role in leaf senescence. *The Plant Journal* **46**, 601–612.
- Han X, Tang S, An Y, et al.** 2013. Overexpression of the poplar NF-YB7 transcription factor confers drought tolerance and improves water-use efficiency in *Arabidopsis*. *Journal of Experimental Botany* **64**, 4589–4601.
- Hiremath PJ, Farmer A, Cannon SB, et al.** 2011. Large-scale transcriptome analysis in chickpea (*Cicer arietinum* L.), an orphan legume crop of the semi-arid tropics of Asia and Africa. *Plant Biotechnology Journal* **9**, 922–931.
- Jia G, Huang X, Zhi H, et al.** 2013. A haplotype map of genomic variations and genome-wide association studies of agronomic traits in foxtail millet (*Setaria italica*). *Nature Genetics* **45**, 957–961.
- Kapoor M, Arora R, Lama T, Nijhawan A, Khurana JP, Tyagi AK, Kapoor S.** 2008. Genome-wide identification, organization and phylogenetic analysis of Dicer-like, Argonaute and RNA-dependent RNA polymerase gene families and their expression analysis during reproductive development and stress in rice. *BMC Genomics* **9**, 451.
- Kim N, Moon SJ, Min MK, et al.** 2015. Functional characterization and reconstitution of ABA signaling components using transient gene expression in rice protoplasts. *Frontiers in Plant Science* **6**, 614.
- Kurkela S, Borg-Franck M.** 1992. Structure and expression of kin2, one of two cold- and ABA-induced genes of *Arabidopsis thaliana*. *Plant Molecular Biology* **19**, 689–692.
- Langdon WB.** 2015. Performance of genetic programming optimised Bowtie2 on genome comparison and analytic testing (GCAT) benchmarks. *BioData Mining* **8**, 1.
- Liu J, Carmell MA, Rivas FV, Marsden CG, Thomson JM, Song JJ, Hammond SM, Joshua-Tor L, Hannon GJ.** 2004. Argonaute2 is the catalytic engine of mammalian RNAi. *Science* **305**, 1437–1441.
- Lu C, Fedoroff N.** 2000. A mutation in the *Arabidopsis* HYL1 gene encoding a dsRNA binding protein affects responses to abscisic acid, auxin, and cytokinin. *The Plant Cell* **12**, 2351–2366.
- Luo D, Xu H, Liu Z, et al.** 2013. A detrimental mitochondrial-nuclear interaction causes cytoplasmic male sterility in rice. *Nature Genetics* **45**, 573–577.
- Mallory A, Vaucheret H.** 2010. Form, function, and regulation of ARGONAUTE proteins. *The Plant Cell* **22**, 3879–3889.
- Ma JB, Yuan YR, Meister G, Pei Y, Tuschl T, Patel DJ.** 2005. Structural basis for 5'-end-specific recognition of guide RNA by the *A. fulgidus* Piwi protein. *Nature* **434**, 666–670.
- Mi S, Cai T, Hu Y, et al.** 2008. Sorting of small RNAs into *Arabidopsis* argonaute complexes is directed by the 5' terminal nucleotide. *Cell* **133**, 116–127.
- Mizoguchi M, Umezawa T, Nakashima K, Kidokoro S, Takasaki H, Fujita Y, Yamaguchi-Shinozaki K, Shinozaki K.** 2010. Two closely related subclass II SnRK2 protein kinases cooperatively regulate drought-inducible gene expression. *Plant & Cell Physiology* **51**, 842–847.
- Muthamilarasan M, Prasad M.** 2015. Advances in *Setaria* genomics for genetic improvement of cereals and bioenergy grasses. *Theoretical and Applied Genetics* **128**, 1–14.
- Nagasaki H, Itoh J, Hayashi K, et al.** 2007. The small interfering RNA production pathway is required for shoot meristem initiation in rice. *Proceedings of the National Academy of Sciences of the United States of America* **104**, 14867–14871.

- Nonomura K, Morohoshi A, Nakano M, Eiguchi M, Miyao A, Hirochika H, Kurata N.** 2007. A germ cell specific gene of the ARGONAUTE family is essential for the progression of premeiotic mitosis and meiosis during sporogenesis in rice. *The Plant Cell* **19**, 2583–2594.
- Qi Y, Denli AM, Hannon GJ.** 2005. Biochemical specialization within *Arabidopsis* RNA silencing pathways. *Molecular Cell* **19**, 421–428.
- Rietz S, Dermendjiev G, Oppermann E, Tafesse FG, Effendi Y, Holk A, Parker JE, Teige M, Scherer GF.** 2010. Roles of *Arabidopsis* patatin-related phospholipases in root development are related to auxin responses and phosphate deficiency. *Molecular Plant* **3**, 524–538.
- Rivas FV, Tolia NH, Song JJ, Aragon JP, Liu J, Hannon GJ, Joshua-Tor L.** 2005. Purified Argonaute2 and an siRNA form recombinant human RISC. *Nature Structural & Molecular Biology* **12**, 340–349.
- Shannon P, Markiel A, Ozier O, Baliga NS, Wang JT, Ramage D, Amin N, Schwikowski B, Ideker T.** 2003. Cytoscape: a software environment for integrated models of biomolecular interaction networks. *Genome Research* **13**, 2498–2504.
- Shinozaki Y, Tanaka T, Ogiwara I, Kanekatsu M, van Doorn WG, Yamada T.** 2014. Expression of an AtNAP gene homolog in senescing morning glory (*Ipomoea nil*) petals of two cultivars with a different flower life span. *Journal of Plant Physiology* **171**, 633–638.
- Song JJ, Joshua-Tor L.** 2006. Argonaute and RNA--getting into the groove. *Current Opinion in Structural Biology* **16**, 5–11.
- Song JJ, Smith SK, Hannon GJ, Joshua-Tor L.** 2004. Crystal structure of Argonaute and its implications for RISC slicer activity. *Science* **305**, 1434–1437.
- Sun W, Meng X, Liang L, Jiang W, Huang Y, He J, Hu H, Almqvist J, Gao X, Wang L.** 2015. Molecular and biochemical analysis of chalcone synthase from *Freesia hybrid* in flavonoid biosynthetic pathway. *PLoS ONE* **10**, e119054.
- Supek F, Bosnjak M, Skunca N, Smuc T.** 2011. REVIGO summarizes and visualizes long lists of gene ontology terms. *PLoS ONE* **6**, e21800.
- Takeda A, Iwasaki S, Watanabe T, Utsumi M, Watanabe Y.** 2008. The mechanism selecting the guide strand from small RNA duplexes is different among argonaute proteins. *Plant & Cell Physiology* **49**, 493–500.
- Takenaka Y, Nakano S, Tamoi M, Sakuda S, Fukamizo T.** 2009. Chitinase gene expression in response to environmental stresses in *Arabidopsis thaliana*: chitinase inhibitor allosamidin enhances stress tolerance. *Bioscience, Biotechnology, and Biochemistry* **73**, 1066–1071.
- Tamura K, Peterson D, Peterson N, Stecher G, Nei M, Kumar S.** 2011. MEGA5: molecular evolutionary genetics analysis using maximum likelihood, evolutionary distance, and maximum parsimony methods. *Molecular Biology and Evolution* **28**, 2731–2739.
- Thompson JD, Gibson TJ, Higgins DG.** 2002. Multiple sequence alignment using ClustalW and ClustalX. *Current Protocols in Bioinformatics Chapter 2*, Unit 2.3.
- Trapnell C, Roberts A, Goff L, Pertea G, Kim D, Kelley DR, Pimental H, Salzberg SL, Rinn JL, Pachter L.** 2012. Differential gene and transcript expression analysis of RNA-seq experiments with TopHat and Cufflinks. *Nature Protocols* **7**, 562–578.
- Vaucheret H.** 2006. Post-transcriptional small RNA pathways in plants: mechanisms and regulations. *Genes & Development* **20**, 759–771.
- Vaucheret H.** 2008. Plant ARGONAUTES. *Trends in Plant Science* **13**, 350–358.
- Voinnet O.** 2009. Origin, biogenesis, and activity of plant microRNAs. *Cell* **136**, 669–687.
- Wang Y, Duan L, Lu M, Li Z, Wang M, Zhai Z.** 2006. Expression of NAC1 up-stream regulatory region and its relationship to the lateral root initiation induced by gibberellins and auxins. *Science in China Series C: Life Sciences* **49**, 429–435.
- Wang Y, Zhang WZ, Song LF, Zou JJ, Su Z, Wu WH.** 2008. Transcriptome analyses show changes in gene expression to accompany pollen germination and tube growth in *Arabidopsis*. *Plant Physiology* **148**, 1201–1211.
- Wu L, Zhang Q, Zhou H, Ni F, Wu X, Qi Y.** 2009. Rice microRNA effector complexes and targets. *The Plant Cell* **21**, 3421–3435.
- Wudick MM, Luu DT, Tournaire-Roux C, Sakamoto W, Maurel C.** 2014. Vegetative and sperm cell-specific aquaporins of *Arabidopsis* highlight the vacuolar equipment of pollen and contribute to plant reproduction. *Plant Physiology* **164**, 1697–1706.
- Xie C, Mao X, Huang J, Ding Y, Wu J, Dong S, Kong L, Gao G, Li CY, Wei L.** 2011. KOBAS 2.0: a web server for annotation and identification of enriched pathways and diseases. *Nucleic Acids Research* **39**, W316–W322.
- Yadav C B, Muthamilarasan M, Pandey G, et al.** 2015. Identification, characterization and expression profiling of Dicer-like, Argonaute and RNA-dependent RNA polymerase gene families in foxtail millet. *Plant Molecular Biology Reporter* **33**, 43–55.
- Yang X, Ren W, Zhao Q, Zhang P, Wu F, He Y.** 2014. Homodimerization of HYL1 ensures the correct selection of cleavage sites in primary miRNA. *Nucleic Acids Research* **42**, 12224–12236.
- Ye R, Wang W, Iki T, Liu C, Wu Y, Ishikawa M, Zhou X, Qi Y.** 2012. Cytoplasmic assembly and selective nuclear import of *Arabidopsis* Argonaute4/siRNA complexes. *Molecular Cell* **46**, 859–870.
- Yu ZX, Wang LJ, Zhao B, Shan CM, Zhang YH, Chen DF, Chen XY.** 2015. Progressive regulation of sesquiterpene biosynthesis in *Arabidopsis* and Patchouli (*Pogostemon cablin*) by the miR156-targeted SPL transcription factors. *Molecular Plant* **8**, 98–110.
- Zhang G, Liu X, Quan Z, et al.** 2012. Genome sequence of foxtail millet (*Setaria italica*) provides insights into grass evolution and biofuel potential. *Nature Biotechnology* **30**, 549–554.
- Zhang S, Tang C, Zhao Q, et al.** 2014. Development of highly polymorphic simple sequence repeat markers using genome-wide microsatellite variant analysis in foxtail millet [*Setaria italica* (L.) P. Beauv.]. *BMC Genomics* **15**, 78.
- Zhang S, Xie M, Ren G, et al.** 2013. CDC5, a DNA binding protein, positively regulates posttranscriptional processing and/or transcription of primary microRNA transcripts. *Proceedings of the National Academy of Sciences of the United States of America* **110**, 17588–17593.
- Zohary D, Hopf M, Weiss E.** 2012. Domestication of Plants in the Old World: The origin and spread of domesticated plants in Southwest Asia, Europe, and the Mediterranean Basin. Oxford: Oxford University Press.